

Performance Evaluation of Geosynthetic Reinforced Pavement Built Over Weak Subgrade Soil using Cyclic Plate Load Test

Murad Abu-Farsakh,¹ Shadi Hanandeh,² Louay Mohammad¹ and Qiming Chen¹

¹*Louisiana Transportation Research Center, Louisiana State University, 4101 Gourrier Avenue, Baton Rouge, LA 70808, USA.*

²*Al Balqa Applied University, Amman, Jordan.*

ABSTRACT

The benefits of using geosynthetics to enhance the performance of pavement constructed over soft subgrade were evaluated using cyclic plate load testing (CPLT). Six test sections, with varying types and layers of geosynthetics and base thicknesses, were constructed inside a 2 m × 2 m × 1.7 m test box. A cyclic load with a frequency of 0.77 Hz was applied through a 305 mm-diameter steel plate. The test sections were instrumented by a variety of sensors to measure the load associated pavement response and performance. The test results clearly demonstrated the benefits of geosynthetic reinforcement in terms of reducing the pavement rutting. The test section with double geosynthetics layers performs much better than the other sections. The geosynthetics placed at the base-subgrade interface function more as stabilization of weak subgrade layer than as base layer reinforcement in this study. Finally, the benefits of geosynthetic reinforcement was quantified, within the context of the AASHTOWare Pavement ME Design guide, in terms of increasing the resilient modulus of base course layer and/or reducing the thickness of base aggregate layer. The results showed that for base reinforcement function alone, the value of resilient modulus of base course layer can be increased by about one quarter, and that the thickness of base layer can be reduced by about one third for the pavement sections with 457 mm thick base and single layer of geosynthetic placed at the base-subgrade interface. For geosynthetics function as subgrade stabilization alone, the test results showed that the resilient modulus of subgrade can be doubled.

Keywords: Geosynthetics, flexible pavement; cyclic plate load tests; traffic benefit ratio, weak subgrade, equivalent modulus, base course reduction.

INTRODUCTION

Weak subgrade soil is a common problem in road construction. Whether it is a temporary access road or a permanent road built over a weak subgrade, a large deformation of the subgrade can lead to deterioration of the paved or unpaved surface. The use of cementitious materials to treat/stabilize the poor subgrade is conventionally accepted practice by many state highway agencies. However, geosynthetics can offer an environmental friendly and potentially economical alternative solution for reinforcing/stabilizing roads built over weak subgrades. The concept of using geosynthetics as reinforcement in roadway construction started in the 1970s.

Since then many experimental, numerical, and analytical studies have been performed to evaluate the benefits of using geosynthetics in pavement application (e.g., Abu-Farsakh et al. 2014; Al-Qadi et al. 1994, 2008; Chen et al. 2009; Kwon et al. 2008; Perkins 2001, 2002). Among various experimental techniques, cyclic plate load test, due to its low cost and time savings, has been widely used by researchers to evaluate the performance of geosynthetic reinforced pavements (e.g., Abu-Farsakh and Chen 2011; Chen et al. 2009; Perkins 1999, 2002; Leng and Gabr 2002; Berg et al. 2000; Al-Qadi et al. 1994). This type of test has also been proved to provide a good performance indicator test for the evaluation of pavement test sections (Chen and Abu-Farsakh 2010).

Two types of geosynthetic products, geotextile and geogrid, are normally used in experimental studies in literature. The results revealed that geosynthetics can extend the service life of a pavement (e.g., Al-Qadi et al. 1997; Cancelli and Montanelli 1999), reduce the thickness of base course layer (e.g., Cancelli and Montanelli 1999), and delay rutting development (e.g., Moghaddas-Nejad and Small 1996). The geosynthetic type and location, base thickness, and subgrade strength have significant effect on the performance of geosynthetic reinforced flexible pavement (e.g., Al-Qadi et al. 2008; Collin et al. 1996; Perkins 1999). Little improvement was obtained for pavement test sections constructed on subgrades with a high California bearing ratio (CBR) values (e.g., Perkins 1999). For a thin base course layer, placing geogrid at the base-subgrade interface gives better performance, while for a thicker course layer, placing the geogrid at the upper one third of the base course layer gives better performance (e.g., Al-Qadi et al. 2008; Haas et al. 1988; Abu-Farsakh and Chen 2011). The benefit of a geosynthetic becomes insignificant if the base course layer is very thick (i.e., greater than 0.6 m) (e.g., Collin et al. 1996).

With pavement design moving toward mechanistic-empirical based methods, quantifying the benefits of geosynthetics and incorporating these benefits into Mechanistic-Empirical Pavement Design Guide (MEPDG) has recently received a lot of attention (e.g., Perkins et al. 2009; Chen and Abu-Farsakh 2012). Nevertheless, a lack of understanding the mechanisms of geosynthetic reinforcement, especially quantifying the geosynthetic benefits, has limited the effectiveness of efforts to change the engineering design practice. These limitations provide a motivation for continual research on geosynthetic reinforced pavements to better understand the geosynthetic reinforcement benefits for incorporating into future pavement design involving mechanistic-empirical pavement design methods.

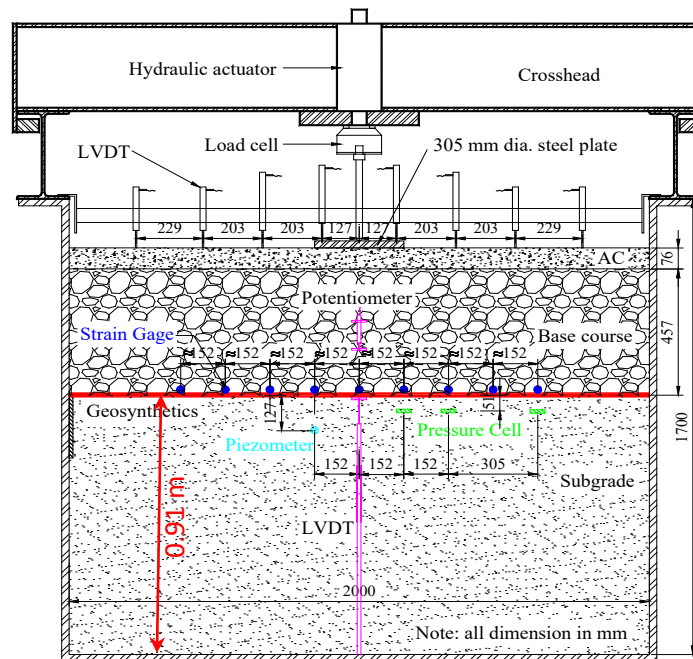
The main objective of this study is to evaluate the benefits of using geogrid and high strength geotextile to reinforce base aggregate layer and/or stabilize weak subgrade soil in flexible pavements. For this purpose, six large-scale laboratory cyclic plate load tests were conducted to examine the effect of geosynthetic types, base course thickness, and number of geosynthetic layers on the performance of geosynthetic reinforced flexible pavement. A variety of sensors was installed for each section to measure the load-associated pavement response and performance, which could be used to quantify the benefits of geosynthetics within the framework of AASHTOWare Pavement ME Design guide.

PAVEMENT TEST SECTIONS

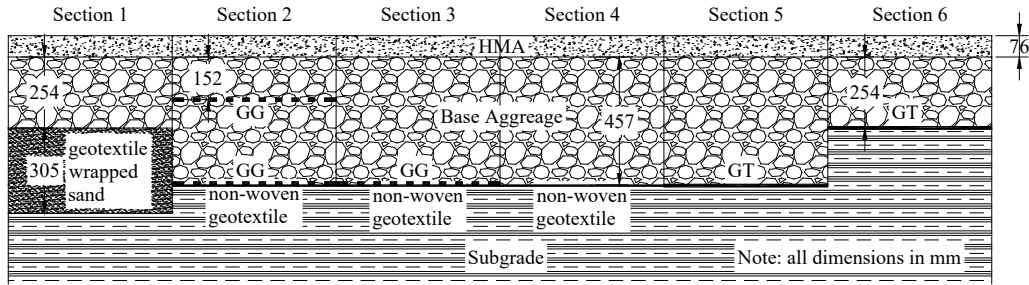
Six large-scale test sections were constructed inside a steel test box with dimensions of 2.0 m (length) \times 2.0 m (width) \times 1.7 m (height). Figure 1a shows a typical box pavement test section with the geometric dimensions and layout of instrumentations used in this study. Each test

section was constructed with 1.06 m of very wet heavy clay to represent the weak natural subgrade soil. The subgrade layer was constructed by mixing the soil with a certain amount of water to achieve the target moisture content with lift thickness of 152 mm. Then, the clay was compacted using a 203-mm × 203-mm plate adapted to a vibratory jack hammer to achieve the desired density. A 305 mm thick geotextile-wrapped sand embankment was then constructed for Section 1. Sections 2 and 3, which have same base layer thickness of 457 mm, were reinforced by triaxial geogrid. While both Sections 2 and 3 have one geogrid layer placed above a nonwoven geotextile at the base-subgrade interface, Section 2 was reinforced with an additional geogrid layer installed at the upper one-third of the base thickness. Section 4 is a control section with 457 mm thick base layer and a layer of non-woven geotextile at the base-subgrade interface. The high-strength woven geotextile, placed at the base-subgrade interface, were used to reinforce Sections 5 and 6, which have base layer thickness of 457 mm and 254 mm, respectively. The thickness of aggregate base was designed based on Giroud Noiray (1981) method for unpaved sections for a number of 80 KN truck passes = 1000 and a rut depth = 2.54 cm (1 in.). Summary of configurations of each test section is shown in Figure 1b.

Various types of instruments were installed at different locations within the pavement layers to measure the load associated pavement response and performance. These include pressure cells to measure the total vertical stress at the top of subgrade layer, piezometer to measure the excess pore water pressure in the subgrade, potentiometer to measure the compressive strain at the mid-height of the base course layer, LVDT to measure the total deformation of subgrade layer, strain gauges to measure the strain distribution along geosynthetics, and LVDTs to measure the surface deformation of pavement test sections. Installation procedures of different instruments can be found in Chen et al. (2009).



(a)



(b)

Figure 1. (a) Indoor test box and load actuator for cyclic load testing and (b) Summary of test sections.

PAVEMENT LAYER MATERIALS

The subgrade soil consisted of a high plasticity clay, having a liquid limit of 88%, a plasticity index of 53%, 96.6 % passing the #200 sieve and an organic content of 9.2%. It is classified as CH per the Unified Soil Classification System (USCS) or A-7-6 according to the American Association of State Highway and Transportation Officials (AASHTO) classification system. The clay has an optimum moisture content of 35% and a maximum dry density of 1,250 kg/m³ according to the standard Procter test. To simulate weak subgrade condition (CBR=0.5), the target moisture content and dry density of subgrade were set as 48% and 1,114 kg/m³, respectively, during construction.

Mexican crushed limestone material was used in the base course layer for all test sections. The crushed limestone had 1.56% passing No. 200 opening sieve, an effective particle size (D_{10}) of 0.382 mm, a mean particle size (D_{50}) of 3.126 mm, a D_{85} of 19 mm, a uniformity coefficient (C_u) of 37, and a coefficient of curvature (C_c) of 3. It is classified as GW and A-1-a according to the USCS and the AASHTO classification systems, respectively. The maximum dry density, as determined by the modified Proctor test is 2,066 kg/m³ at an optimum moisture content of 9.4%. The target moisture content and dry density during construction were set as 7.5% and 1,983 kg/m³, respectively.

The HMA used in the construction is a wearing course. It is a 12.5 mm design level 1 Superpave mixture. The asphalt binder was classified as PG 76-22M according to the Performance Grade (PG) specification. The optimum asphalt binder content is 4.1%. The theoretical maximum density of HMA is 2,480 kg/m³.

Two types of geosynthetics were used in this research, a triaxial geogrid, GG, and a high-strength woven geotextile, GT. The physical and mechanical properties of these geosynthetics as provided by the manufacturer are presented in Table 1.

Table 1. Physical and mechanical properties of geosynthetics used in this study.

Reinforcement	Polymer Type	Tensile Strength, T, (kN/m)		Tensile Modulus, J, (kN/m)		Aperture Size, mm
		MD ^a	CD ^b	MD ^a	CD ^b	
GG	Polypropylene	1.35 ^c		270 ^d		40×40×40
GT	Polypropylene	7.0 ^e	26.3 ^e	350 ^f	1313 ^f	0.425 ^g

^aMachine direction, ^bCross machine direction, ^cTensile strength at 0.5% strain in radial direction, ^dTensile modulus at 0.5% strain in the radial direction, ^eTensile strength at 2% strain, ^fTensile modulus at 2% strain, ^gApparent opening size (AOS).

CYCLIC LOAD TESTING

A hydraulic actuator was used to apply cyclic loads to the pavement test sections through a loading steel plate (25.4 mm thick and 305 mm diameter) sitting on the surface of HMA. The cyclic loading consists of repeated cycles of a loading pulse, which has a linear load increase from 2.2 kN (500 lbf) to the maximum load in 0.3 second, followed by a 0.2-second period the load is held constant. This is, followed by a linear load decrease to 2.2 kN (500 lbf) over 0.3-second period, and then followed by a 0.5-second rest period of 2.2 kN (500 lbf) before the next loading cycle. This results in a loading frequency of 0.77 Hz. The tests were originally designed to apply a maximum load of 40 kN (9,000 lbf) for 100,000 cycles, followed by a maximum load of 53 kN (12,000 lbf) for additional 100,000 cycles, followed by a maximum load of 67 kN (15,000 lbf) for another 100,000 cycles, and then followed by a maximum load of 80 kN (18,000 lbf) for last 100,000 cycles or until reaching 25.4 mm rut depth. However, due to breakdowns of the pump system during testing, the actual load applied never reached the desired maximum loads. The test data for the different sections were converted to Equivalent Single Axle Loads (ESALs) using the AASHTO (2008) fourth power rule equivalency equation follows:

$$ESALs = N \times \left(\frac{Load}{40 \text{ kN}}\right)^4 \quad (1)$$

where N is the number of loading cycles.

TEST RESULTS AND ANALYSIS

Six tests were conducted on different pavement sections, as shown in Figure 1b. The traffic benefit ratio (TBR) was used to evaluate the benefit of geosynthetic reinforcement. TBR is defined as the number of ESALs carried by a reinforced section at a specific rut depth divided by that of an equivalent control section. The results obtained for the different pavement test sections are summarized in Table 2.

EFFECT OF VARIATIONS IN CONSTRUCTED LAYER THICKNESS AND PROPERTIES

As expected in any construction, there are always some variations in the constructed layer thicknesses and properties of the test sections. In order to quantify the effect of differences in the constructed test sections, a relatively simple analysis, using AASHOTOWare Pavement ME Design software (AASHTO 2008), was performed to assess the impact of variations in layer properties and thicknesses, and thereby provide adjustment to the calculated TBR values

(TBR_{adj}). The traffic load was applied using a single tire through special axle configuration available in Pavement-ME software. The load is 40 kN (9,000 lbf) with a tire pressure of 550 kPa (80 psi), which results in a circular loading area of radius 152 mm (6 in). This load magnitude is consistent with that in cyclic plate load tests. The resilient moduli (M_r) for the base and subgrade layer were evaluated using the California bearing ratio CBR-DCPI relationship suggested by Webster et al. (1992) and M_r -CBR relationship suggested by Powell et al. (1992).

$$\left. \begin{aligned} CBR &= 292 / (DCPI)^{1.12} \\ M_r (MPa) &= 17.58 \times CBR^{0.64} \end{aligned} \right\} \Rightarrow M_r (MPa) = 665.06 / (DCPI)^{0.7168} \quad (2)$$

Table 2. Summary of cyclic plate load tests.

Test Sections	Base Thickness (mm)	HMA Thickness (mm)	Rut depth = 12.7 mm		Rut depth = 19.1 mm		Rut depth = 25.4 mm	
			ESALs	TBR	ESALs	TBR	ESALs	TBR
Section 1	451.8	74.1	147290	-	526704	-	1183043	-
Section 2	454.6	76.0	3167943	4.73	-	-	-	-
Section 3	452.1	75.2	822955	1.23	1921712	1.51	3367399	2.19
Control Section 4	459.7	73.6	669960	-	1270908	-	1537749	-
Section 5	447	74.9	800341	1.19	2073279	1.63	3439960	2.24
Section 6	256.5	69.9	20822	-	90483	-	240542	-

The number of ESALs needed to a specific rut depth was calculated for each test section taking into consideration the measured layer's thickness and properties to quantify the effect of construction variations on the analysis of test results. For the reinforced test sections, the comparison was made with respect to its corresponding unreinforced condition, i.e. without geosynthetic reinforcement. The results of the analyses are presented in Table 3. In the table, the variation factor (VF) was introduced to evaluate the effect of differences in constructed layer thickness and properties on the calculated TBR values. The VF is defined here as the number of ESALs at a specific rut depth (i.e., 12.7 mm, 19.1 mm, and 25.4 mm) carried by the corresponding unreinforced condition of the reinforced test section divided by that of the control test section. By dividing the TBR values by the VF factors, the adjusted TBR (TBR_{adj}) was obtained for each reinforced test section and are presented in Table 5. It should be pointed out here that the estimated TBR_{adj} values can be affected by the accuracy of measuring the thicknesses and material properties.

Table 3. Effect of differences in constructed layer properties and thickness.

Test Sections	Rut depth = 12.7 mm			Rut depth = 19.1 mm			Rut depth = 25.4 mm		
	ESALs	VF	$TBR_{adj}^{\#}$	ESALs	VF	$TBR_{adj}^{\#}$	ESALs	VF	$TBR_{adj}^{\#}$
Section 2	39480	1.15	4.11	232800	1.12	-	734400	1.09	-
Section 3	35520	1.03	1.19	211752	1.02	1.48	681600	1.02	2.16
Section 4	34320	-	-	207600	-	-	670800	-	-
Section 5	37200	1.08	1.10	222144	1.07	1.52	710400	1.06	2.11

$^{\#}TBR_{adj} = TBR/VF$

PAVEMENT SURFACE DEFORMATION

Figure 2 illustrates the development of rut depth with number of ESALs for the six pavement test sections. The surface permanent deformation was calculated by averaging the readings of two LVDTs rest on top of the loading plate. The results show that the surface permanent deformation accumulated with the number of ESALs. Sections constructed with geosynthetics experienced less rut depth compared to the control section. More reduction in the pavement surface deformation was observed for the double reinforcement section (Section 2). Sections 3 and 5 can sustain 3,367,399 and 3,439,960 ESALs at a rut depth of 25.4 mm, which result on adjusted traffic benefit ratios (TBR_{adj}) of 2.16 and 2.11, respectively. Section 2, with double reinforced layers, never reached the 25.4 mm rut depth during the test and the rut depth of 12.7 mm was obtained at 3,167,943 ESALs. The performance of Section 1 was much lower than Section 4, which indicates that the 203 mm thick Mexican limestone is more effective than the 305 mm thick nonwoven geotextile-wrapped sand embankment in reducing the pavement rutting. Section 6 showed the lowest performance among the six test sections mainly due to its much thinner base layer (254 mm vs. 457 mm).

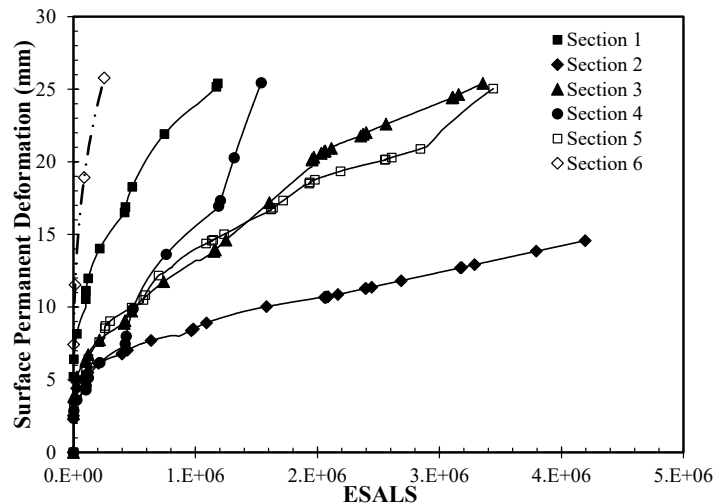


Figure 2. Development of surface permanent deformation.

PERMANENT DEFORMATION IN BASE AND SUBGRADE

As stated earlier, a potentiometer was installed at the mid-height of base layer to measure the compressive strain. It is assumed here that the compressive strain at the mid-height represents the mean compressive strain of the whole layer. As such, the overall deformation of the entire base layer was determined by multiplying the measured compressive strain by the thickness of base layer. In the subgrade layer, an LVDT was mounted on a steel rod, which has an end fixed to the bottom of the steel box. Therefore, the deformation measured by the LVDT is the overall deformation of the entire subgrade layer. Figures 3a and 3b illustrate the development of base and subgrade permanent deformation with number of ESALs. As can be seen from the figures, for the control section (Section 4), the subgrade layer has significant contribution to the total permanent deformation compared to the base layer. The use of geosynthetics resulted in reducing the permanent deformations in both the base and subgrade layers for Sections 2, 3, and 5. However, when the geosynthetic is placed at the base-subgrade interface, significant reduction of

permanent deformation occurred in subgrade layer while only small reduction of permanent deformation was observed in base layer (Section 3 and 5). This means that the geosynthetic at the base-subgrade interface mostly enhance the performance of the weak subgrade, i.e., it functions more as stabilizing the weak subgrade layer than reinforcing the base aggregate layer. For the double reinforced layer (Section 2), the permanent deformations were significantly reduced in both the base and the subgrade layers. This suggests that while the performance of subgrade was significantly improved by the geogrid at the base-subgare interface, the performance of base layer was enhanced by the geogrid placed at the upper one-third of the base layer. Meanwhile, the mesured absolute permanent deformation in the base aggregate layer of Section 1 (relatively weak section) is close to Section 2 due to the use of much thinner base layer in Section 1 (254 mm vs. 457 mm). This means that considerable deformation is expected in the geotextile-wrapped sand layer in Section 1, although no deformation measurement is available for this layer.

STRUCTURAL CONTRIBUTION OF GEOSYNTHETIC REINFORCEMENT

The AASHTOWare Pavement ME Design software was used in this study to analyze the pavement testing sections constructed for CPLTs. The traffic load was applied using a single tire through special axle configuration available in Pavement ME Design software. The load is 40 kN (9,000 lbf) with a tire pressure of 550 kPa (80 psi), which results in a circular loading area of radius 152 mm (6 in). A self-programed climate file was implemented in AASHTOWare to simulate the in-door environmental condition of laboratory CPLTs. The failure criterion of a 19.1 mm (0.75 in) rut depth was used in this study [The failure criterion of 12.7 mm was used (0.5 in) for Section 2 since it never reached 19.1 mm (0.75 in) rut depth]. The benefits of geosynthetics reinforcement were demonstrated through improving the resilient modulus in the mechanistic part of the design. The empirical part available in Pavement ME Design was adopted for both the reinforced and control pavement sections without any change. The geosynthetics have two primary applications in pavement: base reinforcement and subgrade stabilization. When geosynthetics are placed at the base-subgrade interface, the criterion for which function dominates the geosynthetic benefits is difficult to separate. In this paper, the benefit for geosynthetics is evaluated in terms of either of these two functions alone in this study.

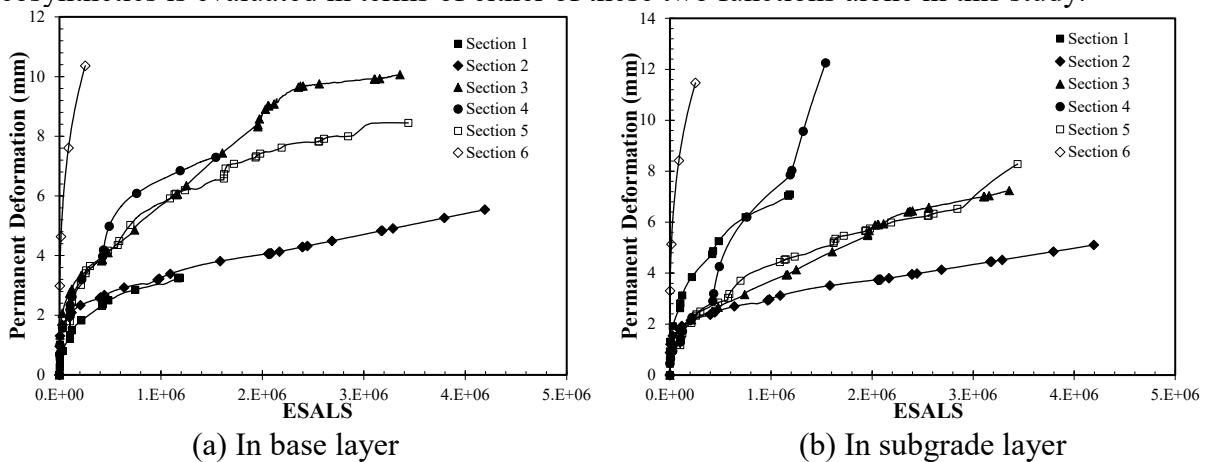


Figure 3. Development of permanent deformation in base and subgrade.

Geosynthetics as base reinforcement. One way to incorporate the benefits of geosynthetic reinforcement into the Pavement ME Design is to adjust the base resilient modulus (M_r) to account for the improved stiffness of the base. In this approach, it is assumed that geosynthetic has no stabilization effect on the subgrade layer, i.e. the subgrade resilient modulus of reinforced sections is kept the same as the corresponding unreinforced condition.

There is a difference between the number of load cycles obtained from the experimental program and that estimated from the Pavement ME Design due to the differences in loading conditions between the plate load test and vehicular loading. As such, a correction factor is needed to account for these differences. This factor was obtained based on the control Section 4 and determined as 6.1. The number of load cycles used in Pavement ME Design is then obtained for reinforced sections by multiplying the number of load cycles obtained from the experimental study by the correction factor. The obtained number of load cycles was then used to back-calculate the effective base resilient modulus for the reinforced sections using the Pavement ME Design software with a failure criterion of a 19.1 mm (0.75 in) rut depth [12.7 mm (0.5 in) for Section 2]. The results of back-calculation are summarized in Table 6. As can be seen from the table, the resilient modulus of the base course layer was increased by 23-25 percent by adding one layer of geosynthetics at the base-subgrade interface, and 82 percent by using two layers of geosynthetics (Section 2). This increase in the base resilient modulus will result in extending the service life of a pavement.

If the service life of the reinforced section is assumed to be the same as that of the unreinforced section, then the base layer thickness can be reduced with the increase of base resilient modulus. This benefit of geosynthetic reinforcement is usually evaluated in terms of the Base Course Reduction (BCR) factor, which is defined as the base thickness of the reinforced section divided by the base thickness of the unreinforced section for a given traffic level. As can be seen from Table 5, the values of BCR range from 0.61 to 0.62 for pavement sections with a single layer of geosynthetics placed at the base-subgrade interface. This means that the thickness of base layer can be reduced by about one third with the inclusion of one layer of geosynthetics placed at the base-subgrade interface. For the pavement section with double layers of geosynthetic reinforcement, the value of BCR is 0.40, which means that a 457 mm (18 inch) thick unreinforced base layer can be reduced to about 203 mm (8 inch) of double-layer geosynthetic reinforced base of same performance. However, this reduction value seems to be not realistic in engineering practice, and should be further investigated.

Table 4. Effective base resilient modulus.

Test Sections	Base Resilient Modulus¹ (MPa)	Effective base Resilient Modulus² (MPa)	Percentage Improvement (%)
Section 2	209	379	82
Section 3	202	250	23
Section 5	208	261	25

¹ $M_r(\text{MPa}) = 665.06 / (\text{DCPI})^{0.7168}$

²Backcalculated from Pavement ME Design software

Table 5. Reduction in base layer thickness.

Test Sections	Base Thickness mm	Reduced Thickness mm	BCR (%)
Section 2	454.6	181.9	40
Section 3	452.1	281.9	62
Section 5	447.0	271.8	61

Geosynthetics as subgrade stabilization. Another approach to incorporate the benefits of placing geosynthetics at the base-subgrade interface within the context of the Pavement ME Design is to adjust the subgrade resilient modulus (M_r) to account for the improved resilient modulus of the subgrade layer (i.e. subgrade stabilization effect). In this approach, it is assumed that geosynthetic has no reinforcement effect on the base layer, i.e., the base course resilient modulus of the reinforced sections is kept the same as its corresponding unreinforced conditions. Again, the Pavement ME Design software was used to back-calculate the effective subgrade resilient modulus for the reinforced sections. The results of back-calculation for Section 3 and 5 are summarized in Table 6. As can be seen from the table, the resilient modulus of subgrade was increased by 87 to 99 percent, depending on the type of geosynthetics. This means that the effective value of subgrade resilient modulus can be almost doubled with the inclusion of a single layer geosynthetic at the base-subgrade interface for pavement sections with 457 mm thick base built over weak subgrade soils.

By assuming that the geogrid at the base-subgrade interface in Section 2 provides the same benefit as that in Section 3 for subgrade stabilization (i.e., 87% increase in subgrade effective resilient modulus), the benefit of geogrid at the upper one third as base reinforcement can then be obtained; which yields an effective base course resilient modulus of 306 MPa (or 47% increase in the base course resilient modulus).

The authors believe that it is more realistic to consider the geosynthetic benefits in terms of increasing the resilient modulus of base course layer than the subgrade layer due to interlocking behavior between geogrids and base aggregate material and possibility of placing geogrids at different locations.

Table 6. Effective subgrade resilient modulus.

Test Sections	Subgrade Resilient Modulus ¹ (MPa)	Effective subgrade Resilient Modulus ² (MPa)	Percentage Improvement (%)
Section 3	17.7	33.1	87
Section 5	17.8	35.5	99

$$^1M_r(\text{MPa}) = 665.06/(\text{DCPI})^{0.7168}$$

²Backcalculated from Pavement ME Design software

CONCLUSIONS

Based on the test results of the cyclic plate load testing program on pavement test sections with and without geosynthetic reinforcement, the following conclusions can be drawn:

- The test results demonstrate that both geosynthetic products significantly improved the performance of the pavement section in terms of reducing the surface permanent deformation

and extending the service life of pavement sections. With a single layer of geosynthetic placed at the base-subgrade interface, the adjusted traffic benefit ratio (TBR_{adj}) can be increased up to 1.52 at a rut depth of 19.1 mm for pavement constructed using 457 mm (18 in.) thick base layer on top of weak subgrade soil.

- Among all six pavement sections tested in this study, the best performance was observed for the pavement section with double geosynthetic reinforcement layers. However, one also should keep it in mind that the cost of having two layers of reinforcement is higher than a single layer of reinforcement.
- The instrumentation measurements indicate that geosynthetics placed at the base-subgrade interface function more as stabilization of weak subgrade soil than as base aggregate reinforcement. By placing an additional geogrid layer at the upper one-third of the base layer, the permanent deformation in base layer can be significantly reduced.
- For geosynthetics function as base reinforcement, within the context of AASHTOWare Pavement ME Design guide, the resilient modulus of base layer can be increased by about one quarter and the thickness of base layer can be reduced by about one-third for the pavement sections tested in this study with 457 mm thick base and a single geosynthetic layer placed at the base-subgrade interface.
- For geosynthetics function as subgrade stabilization, within the context of AASHTOWare Pavement ME Design guide, the resilient modulus of the weak subgrade layer can be almost doubled for the pavement sections tested in this study.

ACKNOWLEDGMENTS

The authors would like to acknowledge the financial support provided by the Louisiana Department of Transportation and Development (LA DOTD), Tensar International., and TenCate. The personnel at Pavement Research Facility of Louisiana Transportation Research Center (LTRC) provided assistance with the accelerated pavement testing. The comments and suggestions of Dr. Zhongjie (Doc) Zhang at LTRC are gratefully acknowledged.

REFERENCES

- AASHTO. (2008). AASHTO Mechanistic-Empirical Pavement Design Guide, Interim Edition: A Manual of Practice, July 2008, American Association of State Highway and Transportation Officials, Washington, DC.
- Abu-Farsakh, M. and Chen, Q. (2011). Evaluation of Geogrid Base Reinforcement in Flexible Pavement Using Cyclic Plate Load Testing.” *International Journal of Pavement Engineering*, 12(275-288).
- Abu-Farsakh, M., Gu, J., Voyiadjis, G.Z. and Chen, Q. (2014). Mechanistic–empirical analysis of the results of finite element analysis on flexible pavement with geogrid base reinforcement. *International Journal of Pavement Engineering*, 15(9): 786-798.
- Al-Qadi, I.L., Brandon, T.L. and Bhutta, S.A. (1997). Geosynthetic stabilized flexible pavements. *Proceedings of the Conference Geosynthetics '97*, Long Beach, CA, USA, March, 1997: 647-661.
- Al-Qadi, I.L., Brandon, T.L., Valentine, R.J., Lacina, B.A. and Smith, T.E. (1994). Laboratory evaluation of geosynthetics reinforced pavement sections.” *Transportation Research Record: Journal of the Transportation Research Board*, No. 1439: 25-31.

- Al-Qadi, I.L., Dessouky, S.H., Kwon, J. and Tutumluer, E. (2008). Geogrid in flexible pavements: validated mechanism. *Transportation Research Record: Journal of the Transportation Research Board*, No. 2045, National Research Council: 102-109.
- Berg, R. R., Christopher, B.R. and Perkins, S.W. (2000). Geosynthetic reinforcement of the aggregate base course of flexible pavement structures. *GMA White paper II*, Geosynthetic Materials Association, Roseville, MN, USA, 100 pp.
- Cancelli, A. and Montanelli, F. (1999). In-ground test for geosynthetic reinforced flexible paved roads. *Proceedings of the Conference Geosynthetics '99*, Boston, MA, USA, April: 863-878.
- Chen, Q. and Abu-Farsakh, M. (2010). Field rutting performance of various base/subbase materials under two types of loading. *Transportation Research Record: Journal of the Transportation Research Board*, No. 2186: 90-100.
- Chen, Q. and Abu-Farsakh, M. (2012). Structural Contribution of Geogrid Reinforcement in Pavement. *GeoCongress 2012*: 1468-1475.
- Chen, Q., Abu-Farsakh, M. and Tao, M. (2009). Laboratory evaluation of geogrid base reinforcement and corresponding instrumentation program, *Geotechnical Testing Journal*, Vol. 32, No. 6.
- Collin, J.G., Kinney, T.C. and Fu, X. (1996). Full scale highway load test of flexible pavement system with geogrid reinforced base courses. *Geosynthetics International*, 3(4): 537-549.
- Giroud, J.P and Noiray, L. (1981). Design of geotextile reinforced unpaved roads. *Journal of Geotechnical Engineering Division*, ASCE, 107(9): 1233- 1254.
- Haas R., Wall, J and Carroll, R.G. (1988). Geogrid Reinforcement of Granular Bases in Flexible Pavements, *Transportation Research Record: Journal of the Transportation Research Board*, No. 1188, TRB, National Research Council, Washington, DC, USA: 19-27.
- Kwon, J., Tutumluer, E. and Konietzky, H. (2008). Aggregate Base Residual Stresses Affecting Geogrid Reinforced Flexible Pavement Response, *International Journal of Pavement Engineering*, 9(4): 275-285.
- Leng, J. and Gabr, M.A. (2002). Characteristics of Geogrid-Reinforced Aggregate Under Cyclic Load, *Transportation Research Record* 1786, Paper No. 02-4091.
- Moghaddas-Nejad, F. and Small, J.C. (1996). Effect of geogrid reinforcement in model track tests on pavements. *Journal of Transportation Engineering*, (122)6: 468-474.
- Perkins, S.W. (1999). Geosynthetic Reinforcement of Flexible Pavements Laboratory Based Pavement Test Sections. *Federal Highway Administration Report FHWA/MT-99-001/8138*, Montana Department of Transportation, Helena, Montana, USA, 109 pp.
- Perkins, S.W. (2001). Mechanistic-empirical modeling and design model development of geosynthetic reinforced flexible pavements. *Federal Highway Administration Report FHWA/MT-01-002/99160-1A*, Montana Department of transportation, Helena, Montana, USA, 126 pp.
- Perkins, S.W. (2002). Evaluation of geosynthetic reinforced flexible pavement systems using two pavements test facilities. *Federal Highway Administration Report FHWA/MT-02-008/20040*, Montana Department of Transportation, Helena, Montana, USA, 120 pp.
- Perkins, S.W., Christopher B.R., Cuelho, E.G., Eiksund, G. R., Schwartz, C.S. and Svanø, G. (2009). A Mechanistic-Empirical Model for Base-Reinforced Flexible Pavements, *International Journal of Pavement Engineering*, 10(2): 101–114.
- Powell, W.D., Potter, J.F., Mayhew, H.C. and Nunn, M.E. (1984). *The Structural Design of Bituminous Roads*. Transport and Road Research Laboratory (TRRL), Report LR1132, Berkshire, United Kingdom.

Webster, S.L., Grau, R.H. and Williams, R.R. (1992). *Description and Application of Dual Mass Dynamic Cone Penetrometer*. U.S. Army Engineer Waterways Experiment Station, Instruction Report, No. GL-92-3.